the plant journal

SEB Society for Experimental Biology

The Plant Journal (2018) **94,** 340–351 doi: 10.1111/tpj.13860

Bifunctional glycosyltransferases catalyze both extension and termination of pectic galactan oligosaccharides

Tomas Laursen[1], Solomon H. Stonebloom[1], Venkataramana R. Pidatala[1], Devon S. Birdseye[1], Mads H. Clausen[2], Jenny C. Mortimer[1] and Henrik Vibe Scheller[1,3,*]

[1]*Joint BioEnergy Institute and Environmental Genomics and Systems Biology Division, Lawrence Berkeley National Laboratory, Berkeley, CA 94702, USA,*

[2]*Department of Chemistry, Center for Nanomedicine and Theranostics, Technical University of Denmark, DK-2800 Kongens LyngbyDenmark, and*

[3]*Department of Plant and Microbial Biology, University of California, Berkeley, CA 94720, USA*

Received 11 December 2017; revised 23 January 2018; accepted 31 January 2018; published online 8 February 2018.
*For correspondence (e-mail hscheller@lbl.gov).

SUMMARY

Pectins are the most complex polysaccharides of the plant cell wall. Based on the number of methylations, acetylations and glycosidic linkages present in their structures, it is estimated that up to 67 transferase activities are involved in pectin biosynthesis. Pectic galactans constitute a major part of pectin in the form of side-chains of rhamnogalacturonan-I. In Arabidopsis, galactan synthase 1 (GALS1) catalyzes the addition of galactose units from UDP-Gal to growing β-1,4-galactan chains. However, the mechanisms for obtaining varying degrees of polymerization remain poorly understood. In this study, we show that *At*GALS1 is bifunctional, catalyzing both the transfer of galactose from UDP-α-D-Gal and the transfer of an arabinopyranose from UDP-β-L-Ara$_p$ to galactan chains. The two substrates share a similar structure, but UDP-α-D-Gal is the preferred substrate, with a 10-fold higher affinity. Transfer of Ara$_p$ to galactan prevents further addition of galactose residues, resulting in a lower degree of polymerization. We show that this dual activity occurs both *in vitro* and *in vivo.* The herein described bifunctionality of *At*GALS1 may suggest that plants can produce the incredible structural diversity of polysaccharides without a dedicated glycosyltransferase for each glycosidic linkage.

Keywords: plant biochemistry, cell wall, glycosyltransferase, biosynthesis, degree of polymerization.

INTRODUCTION

The plant cell wall is a highly complex composite of polysaccharides, lignin and glycoproteins, with an estimated 10% of the genome involved in its biosynthesis, secretion, assembly and remodeling (McCann and Rose, 2010). Despite recent advances in our understanding of cell wall structure (Dick-Perez *et al.*, 2011), the identification and characterization of the enzymes involved in its biosynthesis remain limited (Atmodjo *et al.*, 2013). In order to engineer the cell walls of crop plants to obtain increased nutritional value or produce biofuel and plant-derived chemicals, we need to both expand our knowledge of how the plant cell wall is biosynthesized and elucidate the mechanisms governing its regulation.

Pectin, the most complex class of polysaccharides in nature, comprises up to 35% of the primary cell wall of dicots. Pectin is composed of four major domains: homogalacturonan (HG), rhamnogalacturonan I (RG-I), rhamnogalacturonan II (RG-II), and xylogalacturonan (Harholt *et al.*, 2010). Based on the types of methylations, acetylations and glycosidic linkages found in pectin, it has been estimated that about 67 different transferases are required for its biosynthesis (Mohnen, 2008; Caffall and Mohnen, 2009). RG-I consists of alternating α-L-rhamnose and α-D-galacturonic acid residues in a backbone of the alternating disaccharide repeat of [-4-α-D-GalA-(1,2)-α-L-Rha-1-] moieties substituted with galactan, arabinan and arabinogalactan side-chains (Harholt *et al.*, 2010). Pectic galactan is mainly composed of linear β-(1,4)-linked galactose units (Figure 1), although Type II arabinogalactans with β-(1,3)- and β-(1,6)-linked galactose may also be present. Some β-1,4-galactan side-chains of the RG-I backbone have been shown to contain, in addition to galactose

residues, an occasional internal arabinofuranose (Ara_f) residue, and the galactan side-chains may also be branched with Ara_f or terminated with arabinopyranose (Ara_p) residues (Huisman *et al.*, 2001; Figure 1). Galactose is a hexose amenable for fermentation, hence, biosynthesis of galactan has been a target for optimizing feedstocks for biofuel production (Gondolf *et al.*, 2014). Terminal Ara_p has been suggested to cap and terminate the extension of galactan (Ishii *et al.*, 2005a,b). Therefore, in order to increase the amount of galactan and reduce the amount of arabinose, it is essential to understand the biological function of the different galactan structures, and to identify the enzymes involved in their biosynthesis and regulation.

Biosynthesis of pectin takes place in the Golgi and therefore depends on the availability of substrates. Nucleotide sugars, produced through *de novo* and salvage pathways, are interconverted by the action of enzymes primarily located in the cytosol (Bar-Peled and O'Neill, 2011). Nucleotide sugars are then transported into the Golgi by highly specific nucleotide sugar transporters. In the Golgi lumen, glycosyltransferases catalyze the transfer of sequential sugar moieties to the growing pectic polysaccharides. Biosynthesis of galactan and arabinan with exogenous oligosaccharide substrates was characterized using hypocotyl microsomal fractions from etiolated mung bean (*Vigna radiata*) seedlings. These studies characterized the sequential transfer of Ara_f (Konishi *et al.*, 2006) and single addition of Ara_p to α-L-(1,5)-arabinooligosaccharide substrates (Nunan and Scheller, 2003; Ishii *et al.*, 2005a,b), as well as sequential transfer of Gal (Ishii *et al.*, 2004) and single addition of Ara_p to β-D-(1,4)-galactooligosaccharide substrates (Ishii *et al.*, 2005a,b). More recently, enzymes capable of galactan biosynthesis were characterized in *Arabidopsis thaliana*. UDP-Gal is transported into the Golgi lumen by the UDP-Rha/UDP-Gal transporters (URGTs; Rautengarten *et al.*, 2014), where extension of β-(1-4)-linked galactan is catalyzed by galactan synthase 1 (GALS1; Liwanag *et al.*, 2012). The biosynthetic enzymes catalyzing transfer of Ara to galactan have not been identified. Arabinose is mainly found in plant glycans in the furanose ring configuration (Ara_f) derived from the pyranose precursor (Ara_p). Hence, most arabinosyltransferases are expected to catalyze transfer of Ara_f. ARAD proteins (ARAD1 and 2) form a multiprotein complex (Harholt *et al.*, 2012). These are the only transferases currently known to be involved in arabinan biosynthesis (Harholt *et al.*, 2006). However, their biochemical activities have not been demonstrated *in vitro*.

Pectic polysaccharides are deposited early in the primary cell wall of growing and dividing cells, leading to a middle lamella that is rich in pectin (Keegstra, 2010). Although the exact mechanism remains elusive, pectin plays a role in regulating cell growth and extension (Derbyshire *et al.*, 2007). Pectin was initially thought to provide a soft matrix in which cellulose fibers were embedded; however, increasing data suggest direct interactions to cellulose (Wang *et al.*, 2015) and xyloglucan (Popper and Fry, 2008). To date, most data indicate the importance of HG for coordination between pectin and cellulose (Chebli and Geitmann, 2017). Methylation of HG changes the cross-linking between polymers and thereby the accessibility for polygalacturonases to cleave pectin in response to expansion (Xiao *et al.*, 2014). Furthermore, neutral sugar side-chains such as galactan and arabinan have been shown to non-covalently bind to cellulose microfibrils, and play a role in cross-linking the microfibrils of primary cell walls (Zykwinska *et al.*, 2005, 2007). The arabinan chain length of RG-I, but not galactan, is involved in pollen cell wall development (Cankar *et al.*, 2014). Thus, reorganization of the primary cell wall during plant growth requires modification of pectin. However, the role of galactan and its degree of polymerization (DP) both remain unknown.

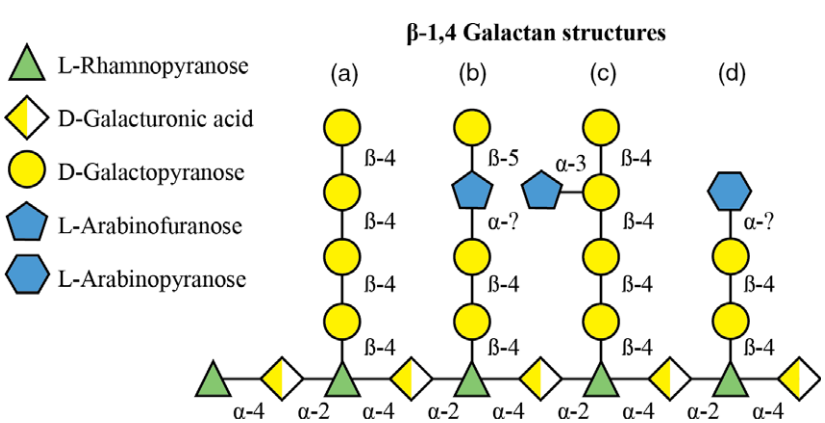

Figure 1. Rhamnogalacturonan I (RG-I) backbone substituted with diverse β-1,4-galactan-rich oligosaccharide side-chains.
RG-I is composed of an alternating backbone of galacturonic acid and rhamnose, which can be substituted with galactan, arabinan and arabinogalactan. Galactan is composed of β-(1,4)-linked galactose units (a), and may contain internal arabinofuranose units (b), branched arabinofuranose units (c) or terminal arabinopyranose units (d). [Colour figure can be viewed at wileyonlinelibrary.com].

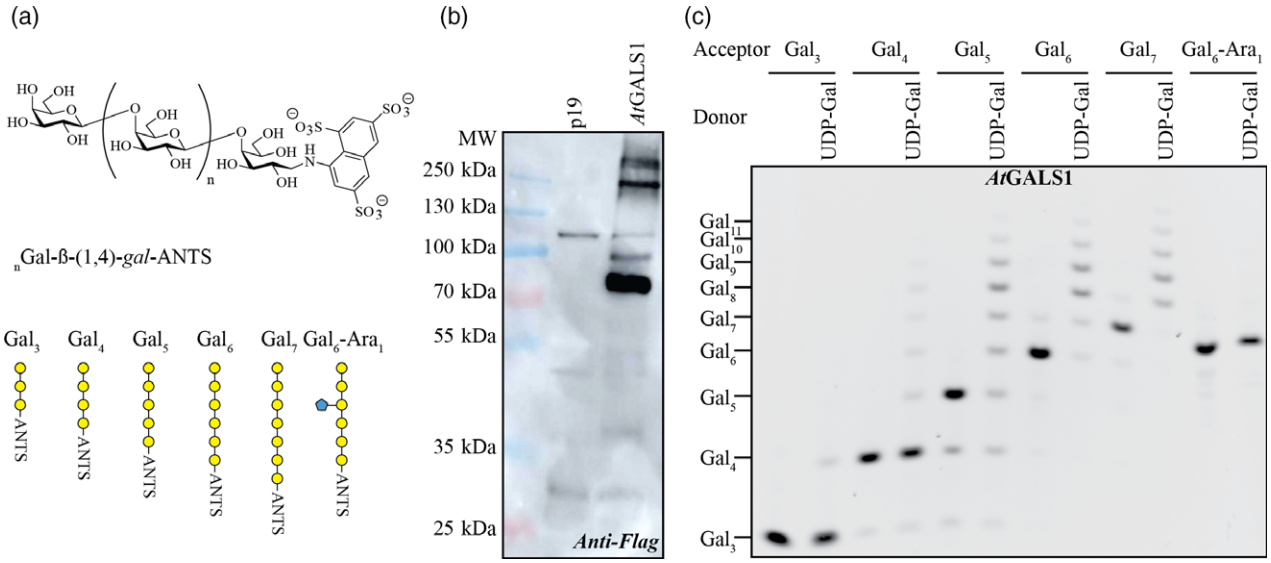

Figure 2. Polysaccharide analysis using carbohydrate gel electrophoresis (PACE).
(a) Several synthetic galactan substrates were reductively labeled with the fluorescent probe 8-aminonaphthalene-1,3,6-trisulfonic acid (ANTS) for PACE assays.
(b) The expression of *At*GALS1, transiently expressed in *Nicotiana benthamiana*, in the microsomal fraction was analyzed by immunoblot using anti-FLAG antibodies, which displayed a distinct band at approximately 70 kDa compared with the p19 background.
(c) PACE assay using *At*GALS1 microsomes and ANTS-labeled substrates in the presence and absence of UDP-Gal as donor sugar displayed a preference for longer galactan substrates ($Gal_{4\text{-}7}$). No conversion was observed in the absence of UDP-Gal. [Colour figure can be viewed at wileyonlinelibrary.com].

In this study, we show that *At*GALS1 is bifunctional, catalyzing the extension of β-(1,4) galactan as well as the termination of extension by addition of Ara_p. These counteracting activities were affected by the availability of nucleotide sugar donors and hence provide a mechanism to alter the formation of specific galactan oligosaccharides. Furthermore, the bifunctionality of GALS1 challenges the paradigm that each glycosidic linkage requires a dedicated transferase. In the case of GALS1, the two substrates are quite similar (Figure S1). We propose that complex cell wall polysaccharides may be biosynthesized by fewer enzymes than initially anticipated (Mohnen, 2008; Caffall and Mohnen, 2009), and that the structure of wall polysaccharides may be influenced by the availability of substrates.

RESULTS

Establishing a method for polysaccharide analysis using carbohydrate gel electrophoresis (PACE)

In order to study the biosynthesis of the different β-(1,4) galactan structures (Figure 1), we labeled chemically synthesized galactooligosaccharide substrates with 8-aminonaphthalene-1,3,6-trisulfonic acid (ANTS) at the reducing end (Figure 2a). Initially, we employed the well-characterized GALS1 from *A. thaliana* (Liwanag *et al.*, 2012) to validate whether labeled galactan substrates (Gal_3, Gal_4, Gal_5, Gal_6, Gal_7 and Gal_6Ara_1) were appropriate substrates for activity studies. Crude microsomes from *Nicotiana benthamiana* leaves transiently expressing *At*GALS1 with an N-terminal FLAG peptide were used as a source of GALS activity. Immunoblot analysis using anti-FLAG antibody verified the expression of *At*GALS1 as compared with control plants expressing p19 alone (Figure 2b). Subsequently, we established the method for PACE to monitor the activity of *At*GALS1, which allowed for the separation of products based on charge and DP (Goubet *et al.*, 2002; Mortimer *et al.*, 2015). Administration of the different galactan substrates with and without UDP-Gal as the donor sugar revealed a preferential activity of *At*GALS1 towards longer substrates ($Gal_{4\text{-}7}$), generating products with a maximum detected DP of approximately 11 (Figure 2c). It is likely that galactans of DP greater than 11 may be synthesized at higher enzyme concentrations and/or substrate concentration or longer reaction times, although this remains to be determined. Branched galactan substituted with an α-(1,6) linked Ara_f at the fourth Gal-position (Gal_6Ara_1) did not serve as substrate for *At*GALS1 (Figure 2c).

Screening of nucleotide sugar donors using mung bean microsomes as model system

We utilized the PACE assay to study the biosynthesis of β-(1,4) galactan structures (Figure 1) using ANTS-labeled galactan substrates (Figure 2a). Previous arabinan and galactan activity studies have been performed using microsomes from etiolated mung bean seedlings. Therefore, we initially verified previously detected activities from mung bean microsomes using Gal_5 as acceptor substrate, and UDP-Gal, UDP-Ara_f or UDP-Ara_p as donor sugars. Under the conditions tested, we detected a ladder of products upon addition of UDP-Gal with a maximum

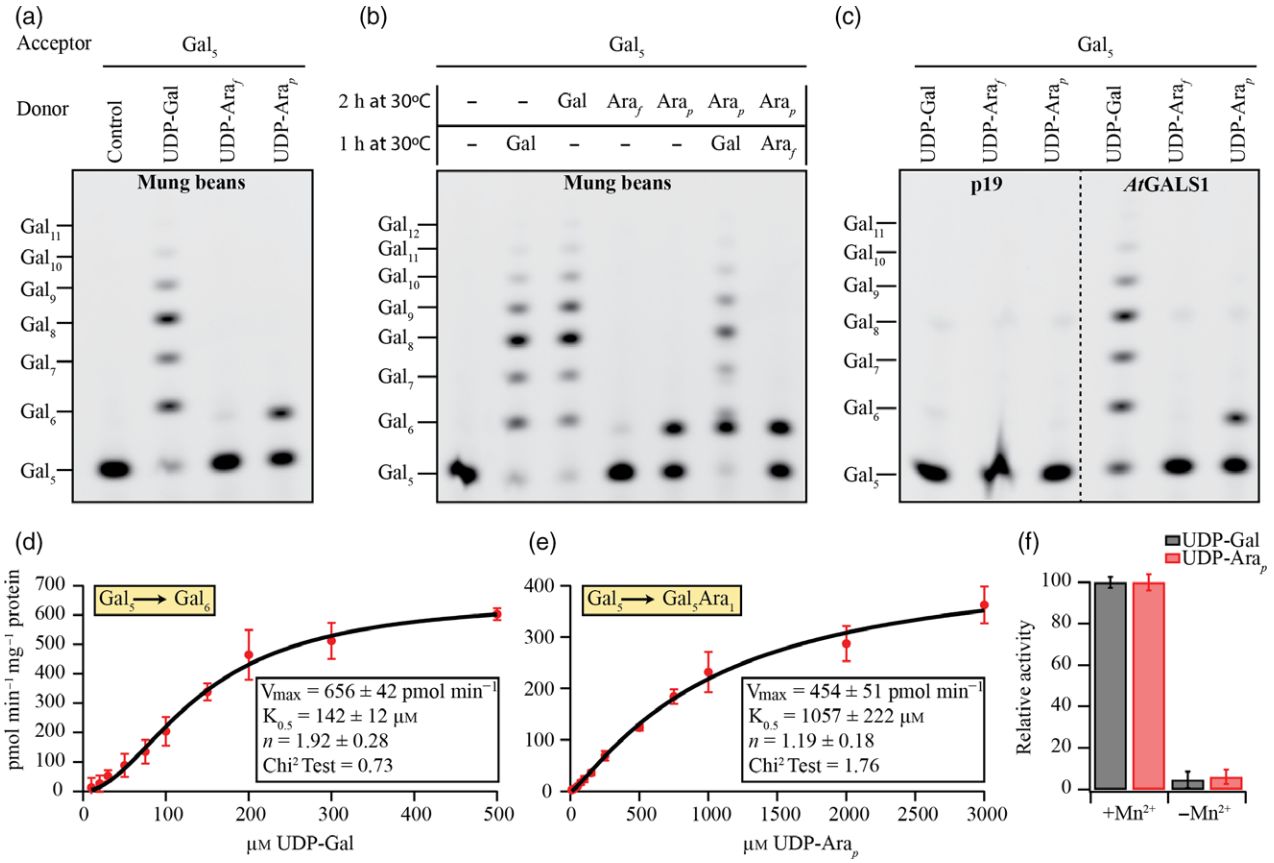

Figure 3. Galactan synthase 1 (GALS1) is bifunctional catalyzing the addition of Gal and Ara_p to galactan substrates.
(a) Polysaccharide analysis using carbohydrate gel electrophoresis (PACE) assay was employed to screen for galactan biosynthetic activities in microsomes prepared from etiolated mung bean hypocotyls using Gal_5 as substrate, and UDP-Gal, UDP-Ara_f or UDP-Ara_p as donor sugars. Administration of UDP-Gal resulted in the formation of a ladder of products, whereas only a single product was formed with UDP-Ara_p. UDP-Ara_f did not serve as donor sugar in this assay.
(b) Sequential activity assay with different donor sugars (listed in the top) supplemented for 2 h followed by administration of a second donor sugar in the same reaction for 1 h (listed below). Sequential addition of UDP-Ara_p followed by administration of UDP-Gal revealed that formation of galactan with a Ara_p served to terminate the growing galactan chain.
(c) *At*GALS1 expressed in *Nicotiana benthamiana* is bifunctional catalyzing the extension of galactan (Gal_5) upon addition of the donor UDP-Gal to the reaction and a single Ara_p extension product upon addition of the donor UDP-Ara_p. UDP-Ara_f did not serve as donor sugar.
(d and e) *At*GALS1 displayed sigmoidal kinetics for both UDP-Gal (d) and UDP-Ara_p (e) as donor sugars using Gal_5 as substrate. Data were fitted to the Hill equation and evaluated based on the Chi^2-test, $K_{0.5}$ represents apparent affinity and n describes the cooperativity for $n > 1$.
(f) Both activities were dependent on divalent cations as demonstrated by supplementation of Mn^{2+}. Values are the average of three technical replicates ± SD. [Colour figure can be viewed at wileyonlinelibrary.com].

oligosaccharide of DP 11 (Figure 3a). Administration of UDP-Ara_p yielded a single product slightly below Gal_6 (Figure 3a). However, administration of UDP-Ara_f did not result in considerable product formation; hence, we were unable to detect the formation of galactan products corresponding to internal or branched Ara_f as previously characterized in soybean pectin (Huisman *et al.*, 2001; Figure 1, structures b and c). Terminal Ara_p has been suggested to cap and terminate the extension of galactan (Ishii *et al.*, 2005a, b; Figure 1, structure d). Therefore, we performed a sequential incubation with UDP-Ara_p followed by the addition of UDP-Gal or UDP-Ara_f (Figure 3b). After the 2-h initial incubation, we supplemented UDP-Gal or UDP-Ara_f to the reactions. Galactan products with the Ara_p did not serve as substrate when UDP-Gal was added as donor sugar, as illustrated by the accumulation of Gal_5Ara_1. The formation of extended galactan oligosaccharides was derived from unmetabolized Gal_5 substrate. Extension of the Gal_5Ara_1 products would have resulted in products with a slightly altered retention compared with $Gal_{(n)}$ products due to the presence of Ara_p. Furthermore, no decrease in the initially formed Gal_5Ara_1 was observed during the subsequent incubation with UDP-Gal. This suggests a fundamental mechanism to affect the DP of galactan by addition of Ara_p to terminate extension (Figure 3b).

*At*GALS1 is bifunctional catalyzing reactions with both UDP-Gal and UDP-Ara_p

As the only characterized glycosyltransferase involved in galactan biosynthesis (Liwanag *et al.*, 2012), we tested the

ability of *At*GALS1 to catalyze the transfer of Gal_p, Ara_f and Ara_p to galactan substrates. As previously shown (Figure 2c), addition of UDP-Gal onto a galactooligosaccharide acceptor of DP≥4 resulted in formation of a ladder of products with a maximum oligosaccharide product DP of 11 (Figure 3c). Interestingly, we consistently observed a predominant formation of Gal_8 products. Upon administration of UDP-Ara_p, *At*GALS1 catalyzed the formation of galactan with a single Ara_p residue (Figure 3c). UDP-Ara_f did not serve as donor sugar when Gal_5 was used as acceptor substrate. *At*GALS1 displayed a similar specificity for long galactan substrates with UDP-Ara_p as donor substrate (Figure S2) compared with UDP-Gal (Figure 2c). In order to validate the biological significance of the UDP-Ara_p activity of *At*GALS1, we determined the kinetic parameters for both UDP-Gal and UDP-Ara_p using Gal_5 as substrate. Both substrates followed sigmoidal kinetics, which were best-fitted to the Hill equation (Figure 3d and e) compared with a hyperbolic fit for enzymes following Michaelis–Menten kinetics based on the Chi^2-test (Figure S3). Sigmoidal kinetics suggests cooperativity related to multiple binding sites or formation of enzyme oligomers (Porter and Miller, 2012). The activity for both UDP-Gal and UDP-Ara_p yielded comparable V_{max} values of 656 and 454 pmol min^{-1} mg^{-1} microsomal protein, respectively. For sigmoidal fits, the apparent substrate affinity is described by the substrate concentration at half-maximum velocity ($K_{0.5}$), which was determined to be 142 and 1057 μM for UDP-Gal and UDP-Ara_p, respectively (Figure 3d and e). Furthermore, the cooperativity of the two donor sugars was evaluated based on the Hill coefficient (n), which describes cooperativity for $n > 1$ (Weiss, 1997). The cooperativity for UDP-Gal showed $n = 1.92 \pm 0.28$, indicating two binding sites for UDP-Gal. For UDP-Ara_p, $n = 1.19 \pm 0.18$, indicating a single binding site for UDP-Ara_p and no significant cooperativity even though the sigmoidal fit was better than the hyperbolic fit. Because the sequence of *At*GALS1 does not indicate the presence of multiple binding sites, the sigmoidal kinetics more likely indicates a multimeric enzyme complex. Both catalytic activities were dependent on divalent cations as tested by the addition or exclusion of Mn^{2+} (Figure 3f).

Nucleotide sugar availability affects galactan DP

Based on the *in vitro* experiments described above, we hypothesized that GALS1 is bifunctional, catalyzing the addition of both Gal and Ara_p to growing galactan chains with DP >3 (Figure S2), and that these counteracting activities are favored by the available pool of donor sugars. We predicted that alteration of the concentration of UDP-Ara_p and UDP-Gal *in vivo* would alter the frequency at which GALS integrates Ara_p into pectic galactans. In order to study the physiological role of GALS1 on pectic galactan DP, we established an *in planta* set-up for altering the intracellular nucleotide sugar levels. In plants, nucleotide sugars are typically derived from UDP-Glc generated through photosynthesis, and the biosynthesis involves a complex grid of interconversions (Bar-Peled and O'Neill, 2011). However, salvage pathways allow uptake of specific sugars, including D-galactose and L-arabinose, which are directly converted into UDP-Gal and UDP-Ara_p, respectively (Bar-Peled and O'Neill, 2011). It has previously been shown that growth of Arabidopsis seedlings on media supplemented with arabinose as a carbon source affects the intracellular concentration of UDP-Ara (Behmuller *et al.*, 2016). To examine the effects of UDP-Ara and UDP-Gal concentration in the nucleotide sugar pool on the biosynthesis of galactans, we grew Arabidopsis seedlings in the dark on media supplemented with sucrose, D-galactose or L-arabinose as the sole carbon source. To test whether possible effects were due to the activity of GALS1, we compared Arabidopsis seedlings of wild-type (Col-0) and GALS1 overexpressor (OE) plants. Seedlings grown with sucrose as the carbon source served as a control for further analyses (Figure 4a). Seedlings grown on D-galactose plates displayed similar growth, with a slight decrease in height for GALS1 OE seedlings compared with Col-0. Both Col-0 and GALS1 OE displayed stunted root growth on D-galactose plates as compared with growth on sucrose. Likewise, seedlings grown on L-arabinose plates displayed stunted root growth and a significant decrease in seedling height for GALS1 OE (Figure 4b). The intracellular nucleotide sugar composition of GALS1 OE seedlings grown on sucrose, D-galactose or L-arabinose was quantified by light chromatography-mass spectrometry/mass spectrometry (LC-MS/MS) and normalized to the seedling fresh weight (Figure 4c). The UDP-Gal/UDP-Glc ratio in seedlings increased from approximately 0.25 when grown on sucrose to 1.95 when grown on D-galactose (Table 1). In contrast, UDP-Gal/UDP-Glc remained unaffected for seedlings grown on L-arabinose plates compared with sucrose plates. However, the UDP-Ara_p/UDP-Glc ratio increased from 0.06 to 0.09 and 0.38 for seedlings grown on sucrose, D-galactose and L-arabinose, respectively (Table 1). These effects correlated with the dramatic increase in intracellular UDP-Gal when seedlings were grown on D-galactose plates and UDP-Ara_p when seedlings were grown on L-arabinose plates. Hence, these sugars were efficiently taken up by the seedlings and converted into activated nucleotide sugars by the salvage pathways (Bar-Peled and O'Neill, 2011).

Nucleotide sugar levels control galactan polymerization mediated by bifunctional GALS

We initially validated the effects of altered intracellular nucleotide sugar concentration (Figure 4c) on cell wall polysaccharide composition by measuring the total monosaccharide composition of alcohol-insoluble residue (AIR) from Col-0 and GALS1 OE. Increasing the intracellular concentration of UDP-Gal and UDP-Ara_p resulted in an

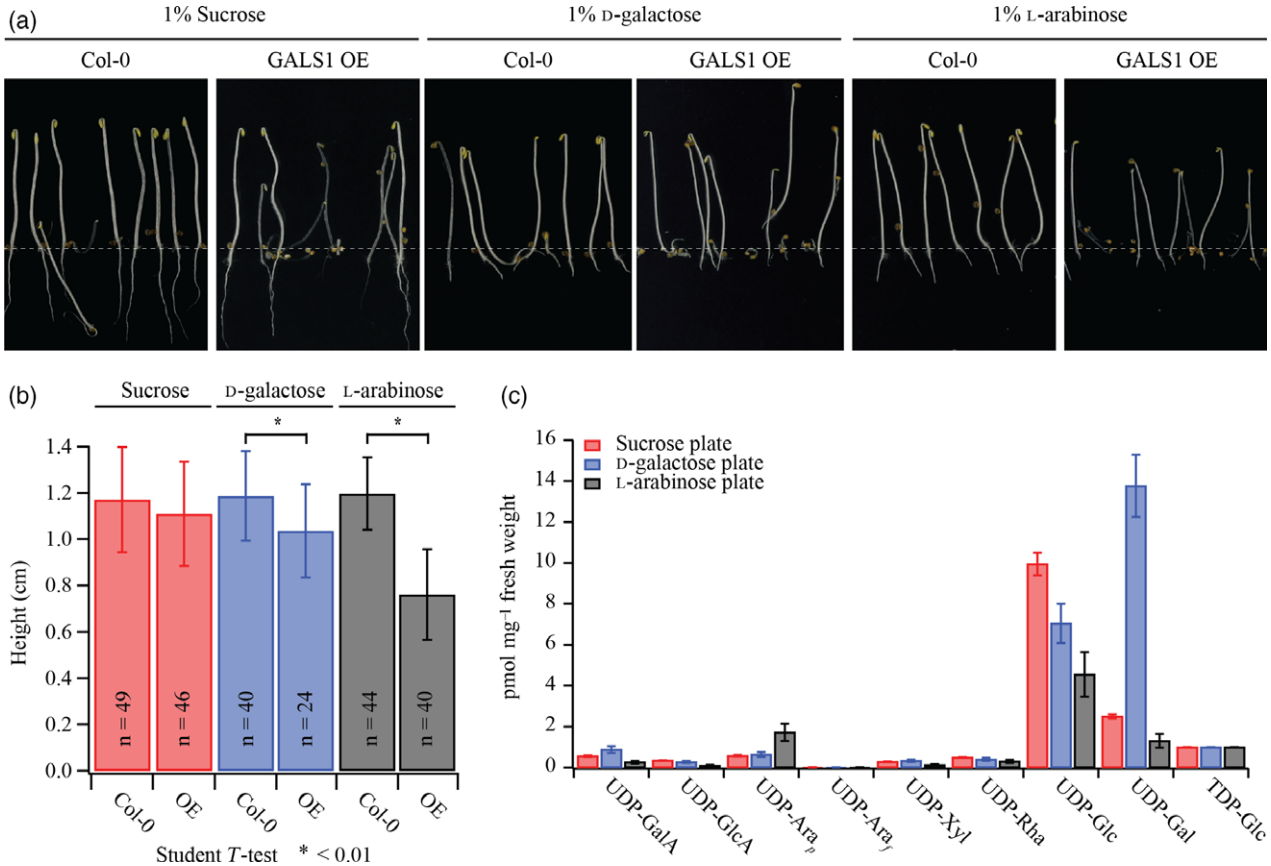

Figure 4. Modifying the intracellular nucleotide sugar concentrations.
(a) Arabidopsis seedlings of wild-type (Col-0) and galactan synthase 1 (GALS1) overexpressor (GALS1 OE) were grown in the dark on plates supplemented with 1% sucrose, 1% D-galactose or 1% L-arabinose.
(b) Col-0 displayed similar seedling height on all sugar plates. GALS1 OE seedlings were slightly shorter when grown on galactose and significantly shorter when grown on arabinose plates compared with seedlings grown on sucrose plates.
(c) Nucleotide sugar analysis of GALS1 OE grown on the different sugar plates revealed an increase in UDP-Gal when grown on galactose plates and an increase in UDP-Ara_p when grown on arabinose plates. This effect is attributed to the salvage pathways for both galactose and arabinose. Values are the average of three technical replicates ± SD. [Colour figure can be viewed at wileyonlinelibrary.com].

increase in total galactose and arabinose content, respectively (Figure S4). We proceeded to analyze the effects on the monosaccharide composition of pectic galactan in both Col-0 and GALS1 OE Arabidopsis seedlings. Galactan was digested by treating the AIR material with *endo*-β-(1,4) galactanase. GALS1 OE seedlings grown on D-galactose plates displayed a significant increase in galactose released by the galactanase treatment, compared with Col-0 and with growth on sucrose media (Figure 5). In contrast, GALS1 OE seedlings grown on L-arabinose plates displayed an increase in solubilized arabinose and a significant decrease in galactose, corresponding to a reduction in galactan production. This supports the hypothesis that addition of Ara_p to galactan serves to terminate extension of the galactan resulting in reduced DP at high concentrations of UDP-Ara_p. We found similar trends for Col-0 seedlings, although the changes in galactan content were not statistically significant. In order to further study galactan DP, we performed glycosyl linkage analysis on isolated RG-I from GALS1 OE seedlings grown on sucrose, D-galactose and L-arabinose (Table 2). DP was evaluated based on the amounts of 1,4-linked galactose (4-Gal), terminal galactose (t-Gal), 1,2-linked rhamnose (2-Rha) and 1,2,4-linked rhamnose (2,4-Rha). We were unable to quantify terminal arabinopyranose. Therefore, based on this study we cannot conclude that the Ara_p is added to the terminal galactose unit of galactans. The ratio 4-Gal/t-Gal represents an estimate of galactan DP containing a terminal galactose unit. Because galactan is a substitution of 2,4-Rha, the ratio 4-Gal/2,4-Rha represents an estimate of the average galactan DP. We want to emphasize that these calculations make several assumptions and are meant for comparison rather than accurate estimates of DP. Seedlings grown on D-galactose plates displayed a dramatic increase in galactan DP with 11.8 4-Gal/t-Gal and 36.1 4-Gal/2,4-Rha compared with 3.0 and 4.6, respectively, for seedlings grown on sucrose (Table 2). In contrast, seedlings grown on L-arabinose plates displayed a reduction in galactan DP with 0.5

Table 1 Nucleotide sugar concentration in GALS1 OE seedlings grown on sugar plates

Nucleotide sugar	Sucrose plates	D-Galactose plates	L-Arabinose plates
UDP-D-GalA	0.56 ± 0.04	0.88 ± 0.16	0.27 ± 0.06
UDP-D-GlcA	0.35 ± 0.01	0.27 ± 0.05	0.11 ± 0.03
UDP-L-Ara_p	0.58 ± 0.04	0.64 ± 0.12	1.72 ± 0.42
UDP-L-Ara_f	Trace	Trace	Trace
UDP-D-Xyl	0.28 ± 0.01	0.34 ± 0.06	0.13 ± 0.03
UDP-L-Rha	0.50 ± 0.01	0.40 ± 0.08	0.30 ± 0.08
UDP-D-Glc	9.95 ± 0.55	7.05 ± 0.96	4.55 ± 1.09
UDP-D-Gal	2.50 ± 0.11	13.77 ± 1.52	1.31 ± 0.34
TDP-D-Glc	1	1	1
Sum	15.74	24.36	9.4
Ratios			
UDP-Gal/UDP-Glc	0.25	1.95	0.29
UDP-Ara_p/UDP-Glc	0.06	0.09	0.38
UDP-Gal/UDP-Ara_p	4.33	21.45	0.76

Seedlings were grown in the dark on plates supplemented with 1% sucrose, D-galactose or L-arabinose as sole carbon source. Samples were spiked with TDP-Glc corresponding to 1 pmol mg^{-1} fresh weight sample. Values are given in pmol mg^{-1} fresh weight and represent three technical replicates ±SD.

4-Gal/t-Gal and 2.0 4-Gal/2,4-Rha (Table 2). This further supports that the specific activity of GALS1 depends on substrate availability, and is capable of utilizing both UDP-Gal and UDP-Ara_p under physiological conditions *in vivo*.

DISCUSSION

Bifunctional galactosyltransferases as a mechanism to obtain galactan diversity

Based on the number of different methylations, acetylations and glycosidic linkages, biosynthesis of pectin is thought to involve more than 67 transferase activities (Mohnen, 2008; Caffall and Mohnen, 2009). This notion is based on the paradigm that each glycosidic linkage requires a dedicated transferase enzyme but, in reality, few of the enzymes have been characterized and it is not clear how broad their specificities are. Here, we present evidence that the structural diversity may be facilitated by glycosyltransferases that can utilize more than one donor nucleotide sugar. Our *in vitro* data provide strong evidence for the bifunctionality of GALS1. GALS1 catalyzes the extension of growing galactan chains; however, in the presence of UDP-Ara_p, GALS1 transfers a single Ara_p residue (Figure 3c), which serves to terminate elongation of the galactan chain (Figure 3b). *In vivo*, this arabinosyltransferase activity results in decreased galactose content in pectin (Figure 5) with reduced DP (Table 2). A previous study supported that GALS1 acts to elongate the growing galactan chains rather than adding the initial galactose substitution on RG-I (Liwanag *et al.*, 2012). This is further reinforced by the preference of GALS1 for galactan substrates with a minimum DP of four Gal units (Figure 2c). Therefore, the number of galactan substitutions on the RG-I backbone is likely unaffected by GALS, and the effects observed in this study may be directly linked to the DP.

Bifunctional galactan synthases have previously been characterized from bacteria catalyzing the formation of galactan with alternating Gal_f-β-(1,5)-Gal_f and Gal_f-β-(1,6)-Gal_f linkages through a single substrate binding pocket (May *et al.*, 2009, 2012; Levengood *et al.*, 2011). This demonstrates the ability of glycosyltransferases to catalyze the transfer of individual monosaccharides with two distinct glycosidic linkages. In contrast, GALS1 catalyzes the transfer of two distinct monosaccharides, namely Gal and Ara_p to pectic galactan. Furthermore, GALS1 displayed sigmoidal kinetics for both UDP-Gal and UDP-Ara_p (Figure 3d), which suggests allosteric binding or formation of multienzyme complexes (Porter and Miller, 2012). The existence of multiple substrate binding sites could provide a mechanism for adding sugar moieties in blocks of two or more in contrast to sequential transfers and explain the predominant formation of Gal_8 oligomers (Figure 3). This is supported by the lower cooperativity for the single transfer of UDP-Ara_p. As a general approach in plants, multifunctional glycosyltransferases could significantly reduce the number of enzymes required for obtaining the impressive diversity of glycosidic linkages in the plant cell wall, giving rise to the diverse functional roles. In the specific case of GALS1, it should be emphasized that UDP-α-D-Gal and UDP-β-L-Ara_p are relatively similar substrates (Figure S1) and the enzyme is able to accommodate both substrates in the donor site, albeit with a preference for UDP-Gal. In contrast, the acceptor site does not have this flexibility as the Ara_p-containing product cannot serve as substrate for further extension with galactose units (Figure 3b). We should point out that it has not been demonstrated in this study that Ara_p is (1,4)-linked to the penultimate Gal, although that would seem most likely.

Galactan composition is modified by the availability of UDP-Gal_p and UDP-Ara_p

Modulation of cell wall glycan biosynthesis may be achieved in many ways. In this study, we showed that availability of UDP-sugars changed the galactan composition facilitated by bifunctional GALS1 (Figure 5). The low affinity for UDP-Ara_p (Figure 3e) combined with the lower intracellular concentration of UDP-Ara_p when seedlings were grown on sucrose (Table 1) suggests that elongation of galactan is the dominant catalytic reaction. The intracellular concentration of nucleotide sugars may be altered through salvage pathways by growing seedlings on Murashige and Skoog (MS) plates supplemented with specific sugars (Figure 4), which altered the specific activity of GALS. *In planta*, other mechanisms are thought to control

Table 2 Linkage analysis of RG-I isolated from etiolated GALS1 OE seedlings

Linkage	Suc 1	Suc 2	Suc Avg.	Gal 1	Gal 2	Gal Avg.	Ara 1	Ara 2	Ara Avg.
t-Ara$_f$	3.0	5.8	4.4	2.0	1.7	1.9	4.1	5.1	4.6
t-Gal	3.5	5.2	4.3	4.5	2.4	3.4	6.9	2.9	4.8
4-Gal	6.0	19.2	12.6	55.1	25.3	40.0	1.1	3.4	2.3
2-Rha	7.0	20.8	13.9	6.2	3.4	4.8	19.3	25.1	22.3
2,4-Rha	1.2	4.4	2.8	0.6	1.9	1.3	0.6	1.7	1.2
3-Ara$_f$	n.d.	n.d.		n.d.	n.d.		n.d.	0.8	0.4
4-Ara$_p$ and 5-Ara$_f$	6.0	6.9	6.5	n.d.	n.d.		7.1	11.3	9.4
t-Xyl	n.d.	n.d.		n.d.	n.d.		n.d.	0.6	0.3
4-Xyl	12.6	9.1	10.9	10.7	2.6	6.7	19.3	6.4	12.5
2,3,4-Xyl	22.3	n.d.	11.2	n.d.	10.3	5.2	9.3	7.6	8.4
3-Gal	10.9	4.8	7.8	1.2	1.9	1.6	n.d.	4.2	2.2
6-Gal	n.d.	n.d.		n.d.	n.d.		n.d.	1.7	0.9
3,6-Gal	1.7	7.9	4.8	n.d.	0.9	0.5	5.8	5.0	5.4
2,3,4,6-Gal	9.9	5.2	7.5	19.6	39.5	29.6	26.4	20.0	23.0
2,3,4-Rha	n.d.	n.d.		n.d.	1.2	0.6	n.d.	1.7	0.9
4-Man	n.d.	n.d.		n.d.	n.d.		n.d.	2.5	1.3
2,3,4,6-Man	15.8	n.d.	7.9	n.d.	8.9	4.5	n.d.	n.d.	
2,3,4-Xyl and 4,6-Glc	n.d.	10.7	5.4	n.d.	n.d.		n.d.	n.d.	
Total	100	100	100	100	100	100	100	100	100
Ratios									
4-Gal/t-Gal			2.9			11.7			0.5
4-Gal/2,4-Rha			4.6			31.6			2.0

RG-I was isolated from etiolated GALS1 OE Arabidopsis seedlings grown on plates supplemented with 1% sucrose, 1% D-galactose or 1% L-arabinose as carbon source. Values are averages of two independent replicates and represented as peak area %; sugars not detected in the analysis are marked with n.d. Ratios indicate the length of galactan chains for seedlings grown on various carbon sources.

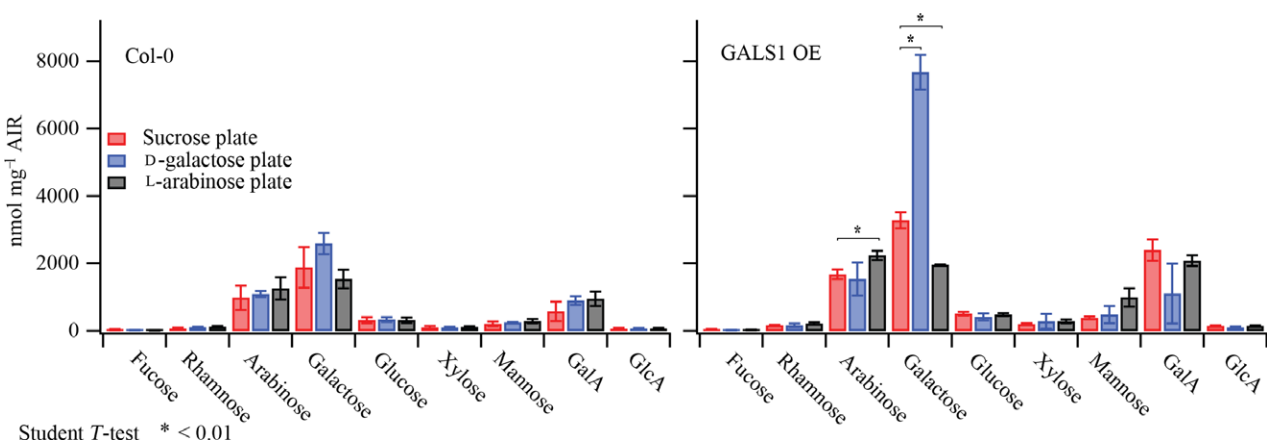

Figure 5. The effect on pectin of seedlings with modified nucleotide sugar levels.
Monosaccharide analysis of the galactan fraction isolated from etiolated Arabidopsis seedlings [Col-0 and galactan synthase 1 (GALS1) overexpressor (OE)] grown on plates supplemented with sucrose, D-galactose or L-arabinose. Values are the average of three technical replicates ± SD. [Colour figure can be viewed at wileyonlinelibrary.com].

the substrate availability, which includes nucleotide sugar mutases and specific Golgi-localized nucleotide sugar transporters. Furthermore, cell wall biosynthesis has been proposed to involve formation of Golgi-localized enzyme complexes, which may have a role in channeling substrates to specific products (Oikawa *et al.*, 2013; Rautengarten *et al.*, 2014). In agreement with this notion, we have observed that knockout and overexpression of URGT1 affected β-(1,4) galactan content without affecting other galactose-containing glycans (Rautengarten *et al.*, 2014). Alternatively, modulating the nucleotide sugar concentrations may provide a key mechanism to alter the composition of the cell wall polysaccharides. In other biosynthesis pathways, dynamic enzyme complexes, metabolons, are known to allow for enzymes to interact transiently and facilitate substrate channeling by increasing the local substrate concentration and direct feeding between sequential enzymes (Laursen *et al.*, 2015, 2016). It is interesting to

speculate that such dynamic complexes could also be involved in generating plasticity in cell wall polysaccharide structures.

In this study, we have demonstrated that growing Arabidopsis seedlings on D-galactose and L-arabinose reduced the intracellular ratio of UDP-Gal/UDP-Ara_p from 21 to 0.8, respectively (Table 1). The relative increase in intracellular UDP-Ara_p resulted in a dramatic decrease in the amount of galactan due to the addition of Ara_p galactan chains (Figure 5). This enables the plant to alter the composition of pectin in response to environmental requirements by modulating the nucleotide sugar concentrations in the Golgi lumen. To date, a specific UDP-Ara_p transporter has not been reported; however, a UDP-GlcA/UDP-GalA transporter (UUAT1) was recently shown to also transport UDP-Ara_p, albeit with lower efficiency (Saez-Aguayo *et al.*, 2017). Accumulation of intracellular UDP-Ara_p correlates with increased Ara in galactan (Figure 5), and therefore suggests a route for UDP-Ara_p to enter the Golgi lumen, possibly through the UUAT1 transporter. Curiously, we did not observe an increase in UDP-Xyl or UDP-Ara_f as would be expected to occur through interconversion of UDP-Ara_p (Bar-Peled and O'Neill, 2011).

Reduction in galactan DP correlated with stunted seedling growth (Figure 4b). However, because GALS mutants with decreased galactan content and decreased DP show no growth phenotype (Liwanag *et al.*, 2012), the observed effect on seedling growth is likely not a direct result of the changes in galactan structure.

Biotechnological applications for optimizing the biosynthesis of linear galactan

In order to optimize the production of galactan for improving feedstocks for biofuel production, we propose an approach to minimize the effect of Ara_p to terminate the extension of linear galactan chains. This may be achieved by modifying the binding site for UDP-Ara_p of GALS1 or alternatively by reducing the Golgi luminal concentration of Ara_p. UDP-xylose-4-epimerase in the Golgi lumen is the key enzyme for producing UDP-Ara_p, but targeting this enzyme may result in a decrease in UDP-Ara_f, which is required for synthesis of many different glycans. Instead, increasing UDP-Ara_p transport out of the Golgi lumen or conversion of UDP-Ara_p to UDP-Ara_f could possibly result in a preferential formation of linear β-(1,4) galactan. This study demonstrates the importance of characterizing all enzymes involved in cell wall biosynthesis and the pitfalls in assuming that glycosyltransferases have a very narrow specificity.

EXPERIMENTAL PROCEDURES

Chemicals

All chemicals were of analytical grade and purchased from Sigma-Aldrich unless otherwise stated. UDP-β-L-Ara_p and UDP-β-L-Ara_f were purchased from Carbosource Service (Complex Carbohydrate Research Center, Athens, GA, USA) and Peptides International (Louisville, KY, USA), respectively.

GALS-FLAG expression in *Nicotiana benthamiana*

Arabidopsis thaliana GALS1 constructs were cloned into pEarleyGate 202 (Earley *et al.*, 2006) containing an N-terminal FLAG tag under the constitutive 35S promoter as described elsewhere (Liwanag *et al.*, 2012). The resulting 35Spro:FLAG-GALS1 construct was transformed into *Agrobacterium tumefaciens* strains GV3101 and used for transient expression in *N. benthamiana*. Leaves of 4-week-old plants were infiltrated with an Agrobacterium strain carrying 35Spro:FLAG-GALS1 (OD_{600} = 0.2) and co-infiltrated with a strain carrying the p19 gene of tomato bushy stunt virus (OD_{600} = 0.2), as described elsewhere (Sparkes *et al.*, 2006). The *N. benthamiana* leaves transiently expressing FLAG-GALS1 were harvested 4 days after infiltration.

Growth of etiolated mung bean seedlings

Mung bean (*V. radiata*) seeds were soaked overnight in deionized water at room temperature in the dark and spread on moist glass wool before being grown for 4 days at 28°C in the dark. The hypocotyls (2 cm in length from the cotyledons) were harvested with a razorblade and used for preparation of microsomal membranes.

Preparation of microsomal membranes

Microsomal membranes were prepared according to the protocol described elsewhere (Nunan and Scheller, 2003). In short, plant tissue was ground in microsomal extraction buffer (50 mM HEPES-KOH pH 7.0, 400 mM sucrose, 20 mM sodium ascorbate, 1 mM PMSF, 1% w/v PVPP). The suspension was filtered through Mira cloth to remove cell debris followed by centrifugation (3000 ***g*** for 10 min). The supernatant was transferred to a new tube and membranes were isolated by centrifugation (100 000 ***g*** for 1 h). The microsomal pellet was resuspended in buffer (50 mM HEPES-KOH pH 7.0, 400 mM sucrose) using a brush and homogenized with a Potter Elvehjem homogenizer (Sigma-Aldrich). Microsomes were flash-frozen and stored at −80°C until use.

ANTS-labeling and analysis of labeled galactan substrates

Linear galactan substrates Gal_n (n = 3–7) and branched Gal_6-Ara_1 were chemically synthesized as described elsewhere (Andersen *et al.*, 2016). Galactan substrates, 200 μg of each oligosaccharide dissolved in H_2O, were reductively aminated with ANTS (Invitrogen) as follows: oligosaccharides were dried on a speedvac and resuspended in 5 μl of 0.2 M ANTS solution (dissolved in 17:3, water:acetic acid), and 5 μl of 0.2 M 2-picoline borane [resuspended in dimethylsulfoxide (DMSO)] was added to each tube, as described in Mortimer *et al.* (2015). Samples were dried and dissolved in 100 μL mQ water. Excess fluorophore was removed using GlykoClean S Cartridges (Prozyme). Labeled oligosaccharides were dried and resuspended to reach 1 μg μl^{-1} and stored at −80°C until use.

Pace

All reactions were performed in a total of 25 μl containing $MnCl_2$ (10 mM), Triton X-100 (1% v/v) in buffer (50 mM MES, pH 6.5). Screening of Gal_n substrates included 2 μg Gal substrate, UDP-sugar (200 μM) and microsomal membranes (50 μg total protein). Reactions were incubated for 2 h at 30°C with agitation (800 rpm). Reactions were terminated by heating (100°C, 3 min), and

precipitated protein and lipids were sedimented by centrifugation (10 000 ***g*** for 10 min). Supernatants (15 μl) were mixed with 15 μl urea (3 M), and the samples (5 μl) were analyzed by separation on large format Tris-borate acrylamide gel prepared as described elsewhere (Goubet *et al.*, 2002), and electrophoresed at 200 V for 30 min followed by 1000 V for 1.5 h. The PACE gels were visualized with a G-box (Syngene, www.syngene.com) equipped with a UV detection filter and long-wave UV tubes (365 nm emission).

Kinetics of UDP-Gal$_p$ and UDP-Ara$_p$

Kinetic measurements of GALS1 transiently expressed in *N. benthamiana* were performed on microsomal membranes. All measurements were performed in the linear range to avoid misinterpretations due to depletion of substrate. Reactions were performed in a total volume of 25 μl containing Gal_5 (50 μM), $MnCl_2$ (10 mM), Triton X-100 (1% v/v) in buffer (50 mM MES, pH 6.5). When UDP-Gal$_p$ was administered as donor sugar reactions were incubated for 15 min under agitation (800 rpm) and contained 1 μg μl^{-1} total microsomal protein and UDP-Gal in concentrations: 0, 10, 20, 30, 50, 75, 100, 150, 200, 300 and 500 μM. When UDP-Ara$_p$ was administered as donor sugar reactions were incubated for 60 min under agitation (800 rpm) and contained 2 μg μl^{-1} total microsomal protein and UDP-Gal in concentrations: 0, 10, 25, 50, 75, 100, 150, 250, 500, 750, 1000, 2000 and 3000 μM.

Products were separated by PACE and quantified using ImageJ software. Data were plotted in Igor Pro (Wavemetrics) and fitted to hyperbolic or sigmoidal equations using built-in fitting parameters and evaluated based on Chi-square test.

Growth of etiolated Arabidopsis seedlings on sugar plates

Arabidopsis seedlings, Col-0 and GALS1 OE were grown on " MS medium plates with 0.7% agar containing 1% sucrose, 1% D-galactose or 1% L-arabinose as the sole sugar source. Seeds were sterilized by incubation in 50% Clorox® Concentrated Regular Bleach, 1% Tween 20 for 5 min, and washed with sterile water prior to plating. Plates were placed at 4°C for 3 days for stratification, and grown at 22°C for 4 days in the dark. Etiolated seedlings were harvested and used for further analyses as described later.

Monosaccharide analysis and galactanase treatment

Alcohol-insoluble residue was prepared as previously described (Harholt *et al.*, 2006), hydrolyzed in 2 M trifluoroacetic acid for 1 h at 120°C, and analyzed by high-performance anion exchange chromatography (HPAEC) as described elsewhere (Øbro *et al.*, 2004).

Isolation of galactan fractions from cell walls of Arabidopsis seedlings grown on sugar plates were prepared by digestion with endo-β-1,4-galactanase (Megazyme, product code E-EGALN) as previously described (Stonebloom *et al.*, 2016). After digestions, the supernatant and pellet were separated by centrifugation and analyzed by hydrolysis in TFA and HPAEC as described above.

Extraction and purification of nucleotide sugars

Extraction of nucleotide sugars from Arabidopsis seedlings was performed according to a previously published protocol (Arrivault *et al.*, 2009). Seedlings were flash-frozen and ground to a powder in a pre-cooled mortar. Powder (30–40 mg) was transferred to a pre-cooled 2-ml Safe-Lock microfuge tube and extracted with 250 μl cold $CHCL_3$/CH_3OH (3:7 v/v). Samples were spiked with 1 pmol TDP-Glc mg^{-1} powder as an internal standard and incubated for 2 h at −20°C. H_2O (200 μl) was then added, and the aqueous upper phase containing soluble nucleotide sugars was collected and transferred to a new tube following centrifugation (420 ***g*** for 4 min). Extraction was repeated twice and the combined aqueous phase containing water-soluble metabolites was dried in a speedvac and resuspended in 1 ml buffer (10 mM ammonium bicarbonate). Nucleotide sugars were purified on reverse phase SPE columns (ENVI-CARB) according to protocol described elsewhere (Rabina *et al.*, 2001). In short, columns were conditioned prior to sample load by addition of 3 ml 60% acetonitrile, 0.3% ammonium formate (pH 9.0), followed by flushing with 3 ml H_2O. Samples were added followed by wash with 3 ml H_2O and 1 ml 60% acetonitrile. Samples were eluted with 3 ml 60% acetonitrile, 0.3% ammonium formate (pH 9.0).

Chromatographic separation and detection of nucleotide sugars

Separation of nucleotide sugars was performed by LC on a 1260 Infinity series HPLC system (Agilent Technologies) with porous graphitic carbon as the stationary phase according to a previously established protocol (Rautengarten *et al.*, 2014), with important modifications. A Hypercarb column (Thermo Scientific; 150 mm × 1 mm, 5 μm) with a Hypercarb guard cartridge (1 mm × 2.1 mm, 5 μm) was used at a flow rate of 100 μl min^{-1} with solvents (A) [water with 0.3% formic acid (pH 9.0) with ammonia, 5% acetonitrile] and (B) (100% acetonitrile). Separation conditions were 100% (vol/vol) A for 5 min, followed by a gradient to 75% (A) in 30 min and then 50% (vol/vol) (A) in 5 min, which was held for a further 5 min before a return to 100% (vol/vol) (A) in 5 min and held for 40 min for reconditioning of the column. The system was run in Micro flow mode with a mix rate of 200 μl min^{-1}, and the column compartment was set to 50°C with samples kept at 10°C. A total of 5 μl of extracted nucleotide sugars spiked with 1 pmol TDP-Glc per mg seedling fresh weight was loaded.

The separated nucleotide sugars were detected using a 4000 QTRAP LC-tandem MS (MS/MS) system (AB Sciex) equipped with a TurbolonSpray (AB Sciex) ion source, essentially as previously reported (Rautengarten *et al.*, 2014). The mass spectrometry parameters are shown in Table S1.

Isolation of RG-I fractions

Rhamnogalacturonan-I fractions were isolated by enzymatic digestion and size-exclusion chromatography, as described elsewhere (Stonebloom *et al.*, 2016).

Glycosyl linkage analysis

Samples were permethylated, depolymerized, reduced and acetylated. The resultant partially methylated alditol acetates (PMAAs) were analyzed by gas chromatography-mass spectrometry (GC-MS), as described elsewhere (Heiss *et al.*, 2009). We detected some glucose linkages, which were assigned to contamination from the dextran-agarose column used for isolation of RG-I and consequently omitted in the data analysis.

About 1.0 mg of the sample was used for linkage analysis. The sample was suspended in 200 μl of DMSO and left to stir for 3 days. Permethylation was performed by two rounds of treatment with sodium hydroxide (15 min) and iodomethane (45 min). After the addition of 2 ml water, residual iodomethane was removed by sparging with nitrogen. The permethylated carbohydrate was extracted with dichloromethane, which was then washed twice with water and evaporated. The permethylated material was hydrolyzed using 2 M TFA (2 h in sealed tube at 121°C), and the acid was removed by repeated evaporation with 2-propanol. The sample was reduced with $NaBD_4$ in 1 M ammonium

hydroxide for 1 h at room temperature. Borate was removed by repeated evaporation with 9:1 methanol-acetic acid and a final evaporation with methanol. The sample was then acetylated using acetic anhydride (250 μl) and TFA (230 μl). After quenching the reaction by addition of 2 ml 0.2 M sodium carbonate, the PMAAs were extracted with 2 ml dichloromethane and analyzed on an Agilent 7890A GC interfaced to a 5975C MSD (mass selective detector, electron impact ionization mode). A 30 m Supelco SP-2331 bonded phase fused silica capillary column was used for separation of the PMAAs.

ACKNOWLEDGEMENTS

This work conducted by the Joint BioEnergy Institute was supported by the Office of Science, Office of Biological and Environmental Research of the US Department of Energy under contract no. DE-AC02-05CH11231 between Lawrence Berkeley National Laboratory and the US Department of Energy. T.L. is recipient of a fellowship awarded by the VILLUM Foundation (95-300-73023). The linkage analysis was supported by the Chemical Sciences, Geosciences and Biosciences Division, Office of Basic Energy Sciences, US Department of Energy grant (DE-SC0015662) to Parastoo Azadi at the Complex Carbohydrate Research Center. M.H.C. is grateful to the Villum Foundation for supporting the PLANET Project. The authors declare no conflict of interest.

AUTHOR CONTRIBUTIONS

T.L., S.H.S. and H.V.S designed the research project. M.H.C. chemically synthesized galactan substrates. T.L., V.R.P. and J.C.M. performed *in vitro* enzyme characterization using the PACE assay. D.S.B. and S.H.S. performed monosaccharide analysis. T.L. and S.H.S. performed nucleotide sugar analysis. T.L., S.H.S. and H.V.S. wrote the manuscript. All authors approved the final manuscript.

SUPPORTING INFORMATION

Additional Supporting Information may be found in the online version of this article.

Figure S1. Haworth projections of α-D-Gal, β-L-Ara$_p$ and β-L-Ara$_f$.

Figure S2. Bifunctional GALS1 display preference for long galactan substrates.

Figure S3. *At*GALS1 kinetics fitted to a hyperbolic curve.

Figure S4. Monosaccharide composition of total AIR preparations from Col-0 and GALS1 OE.

Table S1. LC-MS/MS parameters for nucleotide sugar quantification

REFERENCES

Andersen, M.C., Kracun, S.K., Rydahl, M.G., Willats, W.G. and Clausen, M.H. (2016) Synthesis of beta-1,4-linked galactan side-chains of rhamnogalacturonan I. *Chemistry*, **22**, 11543–11548.

Arrivault, S., Guenther, M., Ivakov, A., Feil, R., Vosloh, D., van Dongen, J.T., Sulpice, R. and Stitt, M. (2009) Use of reverse-phase liquid chromatography, linked to tandem mass spectrometry, to profile the Calvin cycle and other metabolic intermediates in Arabidopsis rosettes at different carbon dioxide concentrations. *Plant J.* **59**, 824–839.

Atmodjo, M.A., Hao, Z. and Mohnen, D. (2013) Evolving views of pectin biosynthesis. *Annu. Rev. Plant Biol.* **64**, 747–779.

Bar-Peled, M. and O'Neill, M.A. (2011) Plant nucleotide sugar formation, interconversion, and salvage by sugar recycling. *Annu. Rev. Plant Biol.* **62**, 127–155.

Behmuller, R., Kavkova, E., Duh, S., Huber, C.G. and Tenhaken, R. (2016) The role of arabinokinase in arabinose toxicity in plants. *Plant J.* **87**, 376–390.

Caffall, K.H. and Mohnen, D. (2009) The structure, function, and biosynthesis of plant cell wall pectic polysaccharides. *Carbohydr. Res.* **344**, 1879–1900.

Cankar, K., Kortstee, A., Toonen, M.A. *et al.* (2014) Pectic arabinan side chains are essential for pollen cell wall integrity during pollen development. *Plant Biotechnol. J.* **12**, 492–502.

Chebli, Y. and Geitmann, A. (2017) Cellular growth in plants requires regulation of cell wall biochemistry. *Curr. Opin. Cell Biol.* **44**, 28–35.

Derbyshire, P., McCann, M.C. and Roberts, K. (2007) Restricted cell elongation in Arabidopsis hypocotyls is associated with a reduced average pectin esterification level. *BMC Plant Biol.* **7**, 31.

Dick-Perez, M., Zhang, Y., Hayes, J., Salazar, A., Zabotina, O.A. and Hong, M. (2011) Structure and interactions of plant cell-wall polysaccharides by two- and three-dimensional magic-angle-spinning solid-state NMR. *Biochemistry*, **50**, 989–1000.

Earley, K.W., Haag, J.R., Pontes, O., Opper, K., Juehne, T., Song, K.M. and Pikaard, C.S. (2006) Gateway-compatible vectors for plant functional genomics and proteomics. *Plant J.* **45**, 616–629.

Gondolf, V.M., Stoppel, R., Ebert, B., Rautengarten, C., Liwanag, A.J., Loque, D. and Scheller, H.V. (2014) A gene stacking approach leads to engineered plants with highly increased galactan levels in Arabidopsis. *BMC Plant Biol.* **14**, 344.

Goubet, F., Jackson, P., Deery, M.J. and Dupree, P. (2002) Polysaccharide analysis using carbohydrate gel electrophoresis: a method to study plant cell wall polysaccharides and polysaccharide hydrolases. *Analyt. Biochem.* **300**, 53–68.

Harholt, J., Jensen, J.K., Sorensen, S.O., Orfila, C., Pauly, M. and Scheller, H.V. (2006) ARABINAN DEFICIENT 1 is a putative arabinosyltransferase involved in biosynthesis of Pectic Arabinan in Arabidopsis. *Plant Physiol.* **140**, 49–58.

Harholt, J., Suttangkakul, A. and Vibe Scheller, H. (2010) Biosynthesis of pectin. *Plant Physiol.* **153**, 384–395.

Harholt, J., Jensen, J.K., Verhertbruggen, Y. *et al.* (2012) ARAD proteins associated with pectic Arabinan biosynthesis form complexes when transiently overexpressed in planta. *Planta*, **236**, 115–128.

Heiss, C., Klutts, J.S., Wang, Z.R., Doering, T.L. and Azadi, P. (2009) The structure of Cryptococcus neoformans galactoxylomannan contains beta-D-glucuronic acid. *Carbohydr. Res.* **344**, 915–920.

Huisman, M.M., Brul, L.P., Thomas-Oates, J.E., Haverkamp, J., Schols, H.A. and Voragen, A.G. (2001) The occurrence of internal (1→5)-linked arabinofuranose and arabinopyranose residues in arabinogalactan side chains from soybean pectic substances. *Carbohydr. Res.* **330**, 103–114.

Ishii, T., Ohnishi-Kameyama, M. and Ono, H. (2004) Identification of elongating beta-1,4-galactosyltransferase activity in mung bean (Vigna radiata) hypocotyls using 2-aminobenzaminated 1,4-linked beta-D-galactooligosaccharides as acceptor substrates. *Planta*, **219**, 310–318.

Ishii, T., Konishi, T., Ito, Y., Ono, H., Ohnishi-Kameyama, M. and Maeda, I. (2005a) A beta-(1→3)-arabinopyranosyltransferase that transfers a single arabinopyranose onto arabino-oligosaccharides in mung bean (Vigna radiate) hypocotyls. *Phytochemistry*, **66**, 2418–2425.

Ishii, T., Ono, H., Ohnishi-Kameyama, M. and Maeda, I. (2005b) Enzymic transfer of alpha-L-arabinopyranosyl residues to exogenous 1,4-linked beta-D-galacto-oligosaccharides using solubilized mung bean (Vigna radiata) hypocotyl microsomes and UDP-beta-L-arabinopyranose. *Planta*, **221**, 953–963.

Keegstra, K. (2010) Plant cell walls. *Plant Physiol.* **154**, 483–486.

Konishi, T., Ono, H., Ohnishi-Kameyama, M., Kaneko, S. and Ishii, T. (2006) Identification of a mung bean arabinofuranosyltransferase that transfers arabinofuranosyl residues onto (1,5)-linked alpha-L-arabino-oligosaccharides. *Plant Physiol.* **141**, 1098–1105.

Laursen, T., Moller, B.L. and Bassard, J.E. (2015) Plasticity of specialized metabolism as mediated by dynamic metabolons. *Trends Plant Sci.* **20**, 20–32.

Laursen, T., Borch, J., Knudsen, C. *et al.* (2016) Characterization of a dynamic metabolon producing the defense compound dhurrin in sorghum. *Science*, **354**, 890–893.

Levengood, M.R., Splain, R.A. and Kiessling, L.L. (2011) Monitoring processivity and length control of a carbohydrate polymerase. *J. Am. Chem. Soc.* **133**, 12758–12766.

Liwanag, A.J.M., Ebert, B., Verhertbruggen, Y., Rennie, E.A., Rautengarten, C., Oikawa, A., Andersen, M.C.F., Clausen, M.H. and Scheller, H.V. (2012)

Pectin biosynthesis: GALS1 in Arabidopsis thaliana is a beta-1,4-galactan beta-1,4-galactosyltransferase. *Plant Cell*, **24**, 5024–5036.

May, J.F., Splain, R.A., Brotschi, C. and Kiessling, L.L. (2009) A tethering mechanism for length control in a processive carbohydrate polymerization. *Proc. Natl Acad. Sci. USA*, **106**, 11851–11856.

May, J.F., Levengood, M.R., Splain, R.A., Brown, C.D. and Kiessling, L.L. (2012) A processive carbohydrate polymerase that mediates bifunctional catalysis using a single active site. *Biochemistry*, **51**, 1148–1159.

McCann, M. and Rose, J. (2010) Blueprints for building plant cell walls. *Plant Physiol.* **153**, 365.

Mohnen, D. (2008) Pectin structure and biosynthesis. *Curr. Opin. Plant Biol.* **11**, 266–277.

Mortimer, J.C., Faria-Blanc, N., Yu, X.L., Tryfona, T., Sorieul, M., Ng, Y.Z., Zhang, Z.N., Stott, K., Anders, N. and Dupree, P. (2015) An unusual xylan in Arabidopsis primary cell walls is synthesised by GUX3, IRX9L, IRX10L and IRX14. *Plant J.* **83**, 413–527.

Nunan, K.J. and Scheller, H.V. (2003) Solubilization of an arabinan arabinosyltransferase activity from mung bean hypocotyls. *Plant Physiol.* **132**, 331–342.

Øbro, J., Harholt, J., Scheller, H.V. and Orfila, C. (2004) Rhamnogalacturonan I in Solanum tuberosum tubers contains complex arabinogalactan structures. *Phytochemistry*, **65**, 1429–1438.

Oikawa, A., Lund, C.H., Sakuragi, Y. and Scheller, H.V. (2013) Golgi-localized enzyme complexes for plant cell wall biosynthesis. *Trends Plant Sci.* **18**, 49–58.

Popper, Z.A. and Fry, S.C. (2008) Xyloglucan-pectin linkages are formed intra-protoplasmically, contribute to wall-assembly, and remain stable in the cell wall. *Planta*, **227**, 781–794.

Porter, C.M. and Miller, B.G. (2012) Cooperativity in monomeric enzymes with single ligand-binding sites. *Bioorg. Chem.* **43**, 44–50.

Rabina, J., Maki, M., Savilahti, E.M., Jarvinen, N., Penttila, L. and Renkonen, R. (2001) Analysis of nucleotide sugars from cell lysates by ion-pair solid-phase extraction and reversed-phase high-performance liquid chromatography. *Glycoconj. J.* **18**, 799–805.

Rautengarten, C., Ebert, B., Moreno, I. *et al.* (2014) The Golgi localized bifunctional UDP-rhamnose/UDP-galactose transporter family of Arabidopsis. *Proc. Natl Acad. Sci. USA*, **111**, 11563–11568.

Saez-Aguayo, S., Rautengarten, C., Temple, H. *et al.* (2017) UUAT1 is a Golgi-localized UDP-uronic acid transporter that modulates the polysaccharide composition of Arabidopsis seed mucilage. *Plant Cell*, **29**, 129–143.

Sparkes, I.A., Runions, J., Kearns, A. and Hawes, C. (2006) Rapid, transient expression of fluorescent fusion proteins in tobacco plants and generation of stably transformed plants. *Nat. Protoc.* **1**, 2019–2025.

Stonebloom, S., Ebert, B., Xiong, G., Pattathil, S., Birdseye, D., Lao, J., Pauly, M., Hahn, M.G., Heazlewood, J.L. and Scheller, H.V. (2016) A DUF-246 family glycosyltransferase-like gene affects male fertility and the biosynthesis of pectic arabinogalactans. *BMC Plant Biol.* **16**, 90.

Wang, T., Park, Y.B., Cosgrove, D.J. and Hong, M. (2015) Cellulose-pectin spatial contacts are inherent to never-dried Arabidopsis primary cell walls: evidence from solid-state nuclear magnetic resonance. *Plant Physiol.* **168**, 871–884.

Weiss, J.N. (1997) The Hill equation revisited: uses and misuses. *FASEB J.* **11**, 835–841.

Xiao, C., Somerville, C. and Anderson, C.T. (2014) POLYGALACTURONASE INVOLVED IN EXPANSION1 functions in cell elongation and flower development in Arabidopsis. *Plant Cell*, **26**, 1018–1035.

Zykwinska, A.W., Ralet, M.C., Garnier, C.D. and Thibault, J.F. (2005) Evidence for *in vitro* binding of pectin side chains to cellulose. *Plant Physiol.* **139**, 397–407.

Zykwinska, A., Thibault, J.F. and Ralet, M.C. (2007) Organization of pectic arabinan and galactan side chains in association with cellulose microfibrils in primary cell walls and related models envisaged. *J. Exp. Bot.* **58**, 1795–1802.

